Three-State Combinatorial Switch Models As Applied to the Binding of Oxygen by Human Hemoglobin†

Martin Straume and Michael L. Johnson*

Department of Pharmacology and Interdisciplinary Biophysics Program, University of Virginia School of Medicine, Box 448, Charlottesville, Virginia 22908

Received April 1, 1987; Revised Manuscript Received September 22, 1987

ABSTRACT: We have generated a series of *all* 6561 unique, discrete three-state combinatorial switch models to describe the partitioning of the cooperative oxygen-binding free change among the 10 variously ligated forms of human hemoglobin tetramers. These models were inspired by the experimental observation of Smith and Ackers that the cooperative free energy of the intersubunit contact regions of the 10 possible ligated forms of human hemoglobin tetramers can be represented by a particular distribution of three distinct energy levels [Smith, F. R., & Ackers, G. K. (1985) *Proc. Natl. Acad. Sci. U.S.A. 82*, 5347–5351]. A statistical thermodynamic formulation accounting for both dimer–tetramer equilibria and ligand binding properties of hemoglobin solutions as a function of oxygen and protein concentrations was utilized to exhaustively test these thermodynamic models. In this series of models each of the 10 ligated forms of the hemoglobin tetramer can exist in one, and only one, of three possible energy levels; i.e., each ligated form was assumed to be associated with a discrete energy state. This series of models includes *all* possible ways that the 10 ligation states of hemoglobin can be distributed into three distinct cooperative energy levels. The mathematical models, as presented here, do not permit equilibria between energy states to exist for any of the 10 unique ligated forms of hemoglobin tetramers. These models were analyzed by nonlinear least-squares estimation of the free energy parameters characteristic of this statistical thermodynamic development. The parameter values and associated variance were determined for each of the 6561 possible three-state combinatorial switch configurations relative to two independent sets of oxygen- and protein-concentration-dependent data [Mills, F. C., Johnson, M. L., & Ackers, G. K. (1976) *Biochemistry 15*, 5350–5362; Chu, A. H., Turner, B. W., & Ackers, G. K. (1984) *Biochemistry 23*, 604–617]. An additional constraint of approximately equal fractional oxygen saturation of tetramer α and β subunits was imposed consistent with independent experimental evidence. The statistical validity of each of the models was characterized for both data sets by the variance ratio obtained from the model-dependent analysis for each configuration relative to the model-independent thermodynamic analysis. Analysis was conducted in two ways such that tetramer α and β subunits were (1) constrained to have equal intrinsic oxygen-binding free energies and (2) permitted to vary independently in their intrinsic oxygen-binding free energies. Extensive grid searches to broadly survey parameter values were performed for each configuration to identify the numerous local minima often encountered. The variance ratios obtained for the three-state combinatorial switch models corresponded to statistically invalid analyses unless the model-dependent free energy values were permitted to assume values that are either physically unrealistic or inconsistent with model-independent thermodynamic observations. However, the inclusion of the quaternary enhancement effect into the formulation of the models is sufficient to enable the models to describe the experimental data with reasonable parameter values.

Human hemoglobin has been studied extensively as a model macromolecular protein assembly exhibiting the property of functional self-regulation. Cooperative changes in the affinity of the tetrameric protein complex for binding oxygen occur as the extent of fractional saturation of available sites is altered (Ackers, 1980; Ackers & Halvorson, 1974; Ackers & Johnson, 1981; Chu et al., 1984; Flanagan et al., 1981; Johnson & Ackers, 1982; Mills & Ackers, 1979; Mills et al., 1976; Pettigrew et al., 1982; Smith & Ackers, 1985). The macroscopic oxygen-binding properties of this system are also sensitive to the total protein concentration by way of the dimer–tetramer equilibrium (Ackers & Johnson, 1981; Johnson & Ackers, 1982; Smith & Ackers, 1985). In addition, the functional behavior of this system is sensitive to the concentrations of small regulatory species present in the environment such as protons, organic phosphates, carbon dioxide, and chloride ions (Johnson et al., 1984). The influences of these multiple regulatory variables are all correlated with each other, making it necessary to consider a multidimensional network of interacting phenomena to fully characterize the functional properties of hemoglobin. Thus, a great deal is known about the behavior of this protein complex with respect to numerous and interrelated regulatory influences on its function. Detailed characterization of this extensively studied system will permit enhanced understanding of the relationships between the structure, energetics, and functional properties of human hemoglobin, in particular, and regulatory proteins, in general.

Of particular interest has been correlation of the thermodynamic description of hemoglobin function with structural properties of the system. X-ray crystallography (Baldwin & Chothia, 1979; Perutz et al., 1969), X-ray absorption fine structure spectroscopy (Eisenberger et al., 1978), resonance

† Supported by National Institutes of Health Grants GM28928 and AM22125.

* Address correspondence to this author.

0006-2960/88/0427-1302$01.50/0

Raman spectroscopy (Asher et al., 1981), and NMR[1] spectroscopy (Russu et al., 1983; Viggiano & Ho, 1979; Viggiano et al., 1979) have all contributed to the base of structural information now known about hemoglobin. Early models that were developed to account for the functional properties of hemoglobin emphasized assignment of detailed protein structural changes to changes in functionally relevant energetic states (Perutz, 1970a,b; Szabo & Karplus, 1972). The concepts employed in developing such models were based largely on intuitive attempts to correlate the structure, function, and energetics of the system. More recent analysis of experimental data that accounts for a number of functionally significant system variables simultaneously (e.g., oxygen concentration, protein concentration, pH, and temperature) has not permitted a satisfactory assignment of atomic level correlations between structure and function according to these earlier models (Chu et al., 1984; Johnson et al., 1984).

Recently, Smith and Ackers (1985) have reported the experimental observation that the cyanomethemoglobin tetramer functions as a three-state combinatorial switch. In these experiments, Smith and Ackers (1985) observed three energetically unique forms of the hemoglobin tetramer. It is important to note that the observation of three energetically distinct forms cannot directly be equated to a statement that the hemoglobin tetramer has three distinct structural forms. The experiments of Smith and Ackers (1985) were, by necessity, conducted on the stable, ligated cyanomet forms of hemoglobin.

The present work describes a rigorous test of a comprehensive series of 6561 unique and discrete three-state combinatorial switch models for hemoglobin binding of oxygen. The generation of these models was inspired by the experimental observations of Smith and Ackers (1985). These tests utilized two independent sets of oxygen-binding data at a variety of total protein concentrations under conditions highly analogous to those of the Smith and Ackers (1985) experiments.

Mathematical Procedures

A mathematical formulation of the thermodynamic linkage scheme characteristic of subunit dissociation and ligand binding based on statistical thermodynamic principles (Johnson & Ackers, 1982; Johnson, 1986) was developed to test *all* 6561 of the unique three-state configurations for the partitioning of the 10 ligation states of hemoglobin tetramers into three distinct energy states. The influence of the dimer–tetramer equilibrium was incorporated to take full advantage of and to accurately account for the information contained in variable protein concentration data. In addition, the data were constrained such that fractional saturation of α and β subunits was approximately equal at two points of tetramer fractional oxygen saturation, consistent with the tolerances derived from the data of Viggiano and Ho (1979). An extensive search of all physically reasonable model parameters (see Uniqueness of Estimated Parameters) was conducted to identify all variance minima for each of the 6561 possible unique three-state configurations. Parameter values determined from independent observations were constrained to their known values. Only the intrinsic free energies for binding oxygen to α or β subunits within the tetramer and the intermediate tetramer cooperative oxygen-binding free energy were variable. This experimental approach permitted assignment of energy values

[1] Abbreviations: EDTA, ethylenediaminetetraacetate; NMR, nuclear magnetic resonance; Tris, tris(hydroxymethyl)aminomethane.

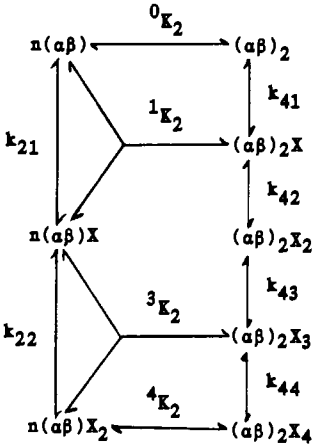

FIGURE 1: Ligand-linked dimer–tetramer association scheme for the binding of oxygen to hemoglobin. k_{2i} and k_{4i} are the stepwise Adair binding constants for each stage of ligation; $^iK_2$ are the equilibrium constants for the formation of tetramers with i oxygens bound; $(\alpha\beta)$ represents hemoglobin dimers; $(\alpha\beta)_2$ represents hemoglobin tetramers; X represents molecules of oxygen bound; n is present to account for the appropriate number of dimers required for stoichiometric balance.

and a corresponding estimate of confidence limits that reflected the validity of a particular analysis. All analyses were characterized by the ratio of the model-dependent variance relative to that of the model-independent thermodynamic analysis as applied to both sets of oxygen-binding data for each three-state configuration examined.

Linkage Scheme. Ligand-linked subunit assembly of human hemoglobin A may be described by Adair constants independent of any specific mechanistic models of hemoglobin action (Johnson et al., 1976; Ackers & Halvorson, 1974). This linkage scheme is presented in Figure 1, where the $^iK_2$ are equilibrium constants for forming tetramers with i oxygens, X_i, bound by combinations of appropriately liganded dimers. The stepwise Adair binding constants, k_{2i} and k_{4i}, are characteristic of forming i-liganded from $(i-1)$-liganded dimers and tetramers, respectively. The product Adair binding constants, K_{2i} and K_{4i}, are the successive products of the stepwise constants, e.g., $K_{43} = k_{41}k_{42}k_{43}$.

The oxygen-binding isotherm for this ligand-linked dimer–tetramer association scheme may be represented mathematically by (Ackers & Halvorson, 1974)

$$\bar{Y}_{2,4} = \frac{Z_2' + [Z_4'\{(Z_2^2 + 4^0K_2Z_4[P_t])^{1/2} - Z_2\}/(4Z_4)]}{Z_2 + (Z_2^2 + 4^0K_2Z_4[P_t])^{1/2}}$$

$$Z_2 = 1 + K_{21}[X] + K_{22}[X]^2$$

$$Z_2' = K_{21}[X] + 2K_{22}[X]^2$$

$$Z_4 = 1 + K_{41}[X] + K_{42}[X]^2 + K_{43}[X]^3 + K_{44}[X]^4$$

$$Z_4' = K_{41}[X] + 2K_{42}[X]^2 + 3K_{43}[X]^3 + 4K_{44}[X]^4$$

$\bar{Y}_{2,4}$ is the fractional oxygen saturation of a system of dimers and tetramers. $[P_t]$ is the total protein concentration (molar heme), and $[X]$ is the concentration of unbound oxygen. $^0K_2$ is the unliganded dimer to unliganded tetramer association constant, and K_{2i} and K_{4i} are the product Adair oxygen-binding constants for dimers and tetramers, respectively.

Discrete Three-State Combinatorial Switch Model. Hemoglobin tetramers may be present in 10 unique ligated forms representing one unliganded form, two singly liganded forms, four doubly liganded forms, two triply liganded forms, and one fully liganded form (see Figure 2) (Smith & Ackers, 1985). The degeneracy present in partially liganded forms results from multiple, nonequivalent ways to distribute bound

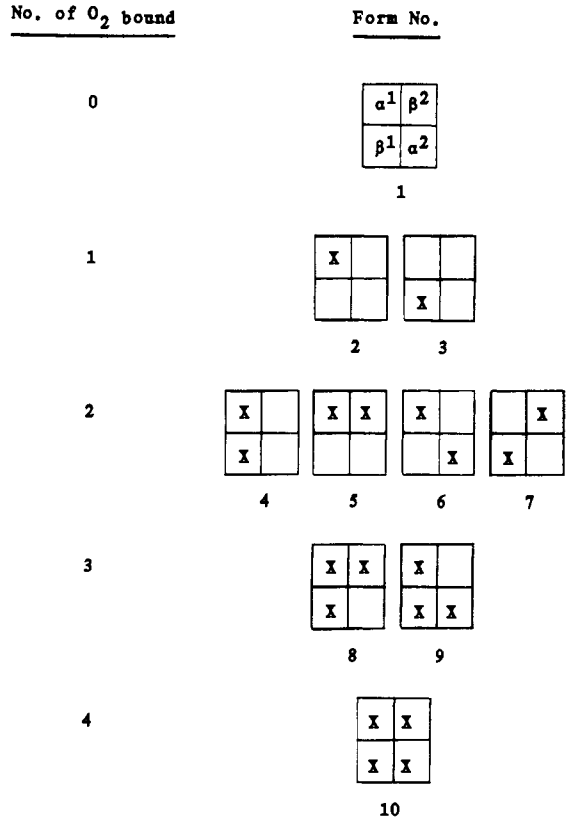

FIGURE 2: Graphic representation of the 10 unique variously ligated forms of hemoglobin tetramers. X represents the presence of oxygen on the labeled subunit. The form numbers correspond to the order of presentation of the 10-digit number representative of a particular configuration of distributed cooperative energy states (form 1 is the left-most digit, form 10 is the right-most digit).

ligand among the α and β subunits of the tetramer. The three-state combinatorial switch model for hemoglobin action involves expenditure of cooperative free energy for binding ligand in two discrete steps, giving rise to three energetically distinct states for the 10 variously ligated tetramers.

Formulation of a mathematical model based on discrete three-state combinatorial switch models involves distribution of three cooperative energy states among the 10 unique forms of variously ligated hemoglobin tetramers. The unliganded tetramer represents the reference state for tetramer cooperative oxygen-binding free energy and is thus constrained to possess zero cooperative free energy. The fully oxygenated tetramer represents another configuration for which the cooperative free energy may be constrained to a known value from independent experimental observations (Mills et al., 1976; Chu et al., 1984). The energy states of two of the 10 unique tetramer forms therefore may be constrained to known values, thus leaving 8 forms among which the three possible energy states are to be distributed. In addition, two of the three cooperative free energy values are determined, leaving the value of only one energy level, the intermediate cooperative oxygen-binding free energy, as a variable.

The configurations of the eight intermediate ligated forms of the tetramer are systematically varied to generate all 6561 possible distributions of the three cooperative oxygen-binding free energies.

Full characterization of oxygen-binding behavior and dimer–tetramer equilibrium distributions of hemoglobin solutions requires knowledge of the oxygen and protein (in terms of molar heme) concentrations and eight parameters descriptive of the thermodynamic linkage scheme. The eight thermodynamic parameters are (1) the unliganded dimer to unliganded tetramer association free energy, (2, 3) the free energies for binding the first and second oxygens to dissociated dimers, (4) the cooperative free energy of the unliganded tetramer, (5) the cooperative free energy of the fully liganded tetramer, (6) the intermediate tetramer cooperative free energy, and (7, 8) the intrinsic oxygen binding free energies for the α and β subunits of tetramers. The unliganded dimer to unliganded tetramer association free energy (1) has been determined independently (Mills et al., 1976; Chu et al., 1984), and the known value is used in analysis. The free energies for binding the first and second oxygens to dissociated dimers (2, 3) have also been determined independently (Mills et al., 1976; Chu et al., 1984) and indicate no cooperativity of oxygen binding to dimers. The known values are used in analysis. The cooperative free energy of the unliganded tetramer (4) serves as the tetramer reference state and thus, by definition, has a value of zero. The cooperative free energy of the fully liganded tetramer (5) has been determined independently (Mills et al., 1976; Chu et al., 1984), and the known value is used in analysis. The intermediate cooperative oxygen binding free energy (6) is a variable in analysis as are the intrinsic oxygen-binding free energies for the α and β subunits in tetramers (7, 8). Analysis is performed under conditions in which the intrinsic oxygen-binding free energies of α and β subunits in tetramers are constrained to be equal as well as under conditions in which they may freely vary independently of each other.

The tetramer configurations are characterized by a 10-digit, base three number, e.g., 1222233333, in which the value of each digit represents cooperative energy state 1, 2, or 3 and the position of the digit corresponds to the tetramer form in the associated energy state. The left-most digit represents the unliganded tetramer (always in state 1), and the right-most digit represents the fully liganded tetramer (always in state 3). The order of the remaining forms is as presented in Figure 2 and Smith and Ackers (1985). The example 1222233333 is the representation corresponding to the configuration deduced by Smith and Ackers (1985) for cyanomethemoglobin.

Uniqueness of Estimated Parameters. The parameter estimation procedure requires initialization by input of some set of initial guess parameter values. The existence of multiple minima raises the possibility of convergence to only one of the multiple local minima that may be present (Johnson & Ackers, 1982; Johnson et al., 1984). For this reason, an extensive grid search of parameter values is employed to select the set of estimated parameters corresponding to the lowest obtainable variance for each tetramer configuration examined.

The intrinsic tetramer α and β subunit oxygen-binding free energies are varied from -12 to -3 kcal/mol, and the intermediate cooperative oxygen-binding free energy is varied from -1 to 11 kcal/mol at 0.5 kcal/mol intervals. This generates a $19 \times 19 \times 25$ grid of possible parameter values containing 9025 elements. The variance is calculated at each of these 9025 grid elements for each tetramer configuration examined relative to the four free energies corresponding to the tetramer product Adair constants known from model-independent thermodynamic analysis. Values of the variance are thus assigned to each element of the grid. Nearest-neighbor comparisons are performed among the variances for each of the 9025 grid elements to identify all loci that represent local minima. Assignment of a near infinite variance to 2882 peripheral grid elements is utilized to facilitate identification of local minima that may be present at the edge elements of the $19 \times 19 \times 25$ grid. After all local minima are identified at 0.5 kcal/mol resolution, variances are calculated around each

identified minimum to a resolution of 0.25 kcal/mol. Each of the sets of parameter values that correspond to local grid minima at 0.25 kcal/mol resolution are then used as initial guesses in the least-squares parameter estimation algorithm (see Appendix). This process is carried out for each of the configurations examined.

Experimental Oxygen-Binding Data Employed. Testing of the statistical thermodynamic models based on discrete three-state combinatorial switch models is performed by analysis of the binding of oxygen to stripped human hemoglobin A as a function of both oxygen and protein concentration in two independent data sets (Mills et al., 1976; Chu et al., 1984). These sets of data include independent evaluations of the dimer to tetramer association constants for both unliganded and fully liganded hemoglobin (Mills et al., 1976; Chu et al., 1984). The experimental conditions under which the oxygen-binding data were collected are 0.1 M Tris, 0.1 M NaCl, and 1.0 mM Na_2EDTA, pH 7.4 (adjusted with concentrated HCl) at 21.5 °C.

Determination of oxygen-binding behavior at various hemoglobin concentrations permits analytical characterization of the influence of the dimer–tetramer equilibrium simultaneously with that of ligand association. Such simultaneous analysis permits better determination of total system properties than would parallel, independent analyses.

All analyses are performed on the actual oxygen-binding data rather than on derived thermodynamic parameters or data synthesized from such derived parameters. This permits direct access to the observed experimental data with associated uncertainties as encountered during data acquisition. The actual experimental data does not contain any of the biases that may have been introduced by intermediate levels of analysis. Each of the oxygen-binding data points have equal statistical weights assigned to them such that the model-independent thermodynamic analysis yields a variance of 1.0 for each data set. Variances derived from model-dependent analyses then directly correspond to the variance ratios of model-dependent to model-independent thermodynamic analysis.

High-resolution ^1H NMR spectroscopy monitoring two hyperfine shifted proton resonances and two exchangeable proton resonances as a function of hemoglobin oxygenation has detected no apparent preferential oxygen binding to the α or β subunits of hemoglobin tetramers (Viggiano & Ho, 1979). These results were included in our analysis by constraining α and β subunits of tetramers to experience approximately equal fractional oxygen saturation at two points in the tetramer oxygen-binding isotherm with approximate standard errors of 5% uncertainty included as reported by Viggiano and Ho (1979). This property of tetramer oxygen-binding behavior is thus accounted for during analysis by statistically constraining the ratio of tetramer α and β subunit oxygen binding according to these independently determined observations.

An appendix has been included to provide details of the statistical thermodynamic formulation of the three-state combinatorial switch models and the nonlinear least-squares parameter estimation procedures.

Results and Discussion

Smith and Ackers (1985) recently reported that cyanomethemoglobin tetramers expend ligand binding cooperative free energy in two steps, thus requiring three distinct energetic states. The experiments of Smith and Ackers (1985) were conducted on hemoglobin ligated at various levels with CN, generating a stable protein–ligand complex required by their experimental protocol.

The particular three-state combinatorial switch configuration reported by Smith and Ackers (1985) corresponds to 1222233333 in the notation of this paper. In their more recent work they have indicated that 1222333333 is possibly a more realistic configuration (Perrella et al., 1987).[2] Neither of these configurations is able to accurately describe either the Mills et al. or Chu et al. oxygen-binding data. Variance ratios[3] of 4.01 and 10.39 were obtained for the analysis of the Mills et al. and Chu et al. data, respectively, by the 1222233333 configuration. Variance ratios of 3.85 and 9.92 were obtained for the analyses of the Mills et al. and Chu et al. data, respectively, by the 1222333333 configuration. Variance ratios of this magnitude correspond to a vanishingly small probability ($P \ll 0.1\%$) of a reasonable fit of the experimental data since the number of degrees of freedom for each of these analyses is approximately 250.

The use of CN as the ligand employed in the experiments of Smith and Ackers (1985) therefore appears to be responsible for quite different qualities in the energetic states of hemoglobin tetramers from those present in the case for oxygen binding. Ackers and Smith (1987) reach a similar conclusion by consideration of binding isotherms and population distributions generated from the data derived from their cyanomethemoglobin experiments. The binding isotherm has a shape quite different from that observed with oxygenation data. A much larger fraction of doubly ligated tetramers is predicted by the cyanomethemoglobin results than from analysis of oxygenation data. Consequently, we decided to investigate all of the other 6559 configurations to determine if *any* of these ways of partitioning the intermediate state cooperative free energy according to a discrete three-state combinatorial switch mechanism are consistent with the oxygen-binding data.

In this paper we have generated a comprehensive series of *all* 6561 unique, discrete three-state combinatorial switch models and have tested these models by a model-dependent, nonlinear least-squares analysis of Mills et al. (1976) and Chu et al. (1984) sets of hemoglobin oxygen-binding data over a range of oxygen and hemoglobin concentrations. A further constraint is imposed on system behavior requiring α and β subunits of the tetramer to experience approximately equal fractional oxygen saturation at two points along the oxygen-binding isotherm as reported by Viggiano and Ho (1979).

Thorough characterization of discrete three-state combinatorial switch models for hemoglobin action theoretically requires the examination of 3^{10} or 59049 distinct combinations of three cooperative energy states distributed among the 10 distinguishable forms of variously ligated hemoglobin tetramers. The unliganded tetramer serves as the cooperative energy reference state and thus is characterized by an invariant energy state (state 1) with known cooperative energy (set to zero by definition). The fully liganded tetramer represents another form with an invariant energy state (state 3) that possesses approximately 6.3–6.4 kcal/mol of cooperative oxygen-binding free energy relative to the unliganded, reference tetramer form (Mills et al., 1976; Chu et al., 1984). The problem is thus reduced to examination of, at most, 3^8 or 6561 distinct combinations of three states among the 8 remaining, intermediately liganded tetramer forms.

Each of these 6561 unique tetramer configurations was examined by employing a grid search over what are deemed

[2] M. Perrella, L. Benazzi, L. Sabbioneda, M. Shea, and G. K. Ackers, personal communication.

[3] For this application the variance ratio is the ratio of the model-dependent variance to the variance of the model-independent thermodynamic analysis.

Table I: Two-Parameter, Three-State Least-Squares Results for the 1223333333 Configuration[a]

parameter	Mills et al. data	Chu et al. data
variance ratio	1.452	3.090
	$P \sim 0.2\%$	$P \sim 0$
$\Delta g_{21}' = \Delta g_{22}'$	−8.410	−8.323
$E(\alpha,\text{tet})$	−8.401 ± 0.001	−8.303 ± 0.001
$E(\beta-\alpha,\text{tet})$	0	0
$E(\text{coop},2)$	3.020 ± 0.024	2.931 ± 0.021
$E(\text{coop},3)$	6.359	6.330
$^0\Delta G_2$	−14.437	−14.421

[a] Variance ratio = F-statistic = (model-dependent variance)/(model-independent thermodynamic variance); $\Delta g_{21}' = \Delta g_{22}'$ = intrinsic dimer subunit oxygen-binding free energy; $E(\alpha,\text{tet})$ = intrinsic tetramer α subunit oxygen-binding free energy; $E(\beta-\alpha,\text{tet})$ = difference between intrinsic tetramer β and α subunit oxygen-binding free energies; $E(\text{coop},2)$ = intermediate tetramer cooperative oxygen binding free energy; $E(\text{coop},3)$ = unliganded to fully liganded tetramer cooperative oxygen-binding free energy, i.e., $^4\Delta G_2 - {}^0\Delta G_2$; $^0\Delta G_2$ = unliganded dimer to unliganded tetramer association free energy; P = probability as derived from values of the variance ratio (F-statistic) for 236 data points (Mills et al. data) and 283 data points (Chu et al. data). The configuration reported corresponds to the order of tetramer forms as reported in Figure 2 and Smith and Ackers (1985), and the rigidly constrained parameter values correspond to the optimal, independently determined quantities for $E(\text{dimer})$, $E(\text{coop},3)$, and $^0\Delta G_2$ for the respective data sets. All energies in kilocalories per mole.

physically reasonable parameters (as described under Uniqueness of Estimated Parameters) to identify all local minima relative to the known macroscopic tetramer product Adair constants. Parameter values corresponding to these grid minima are subsequently used as initial guesses in the least-squares parameter estimation process (see Appendix). This grid search facilitates identification of the variance minimum for each configuration examined. This is important as up to approximately 30 local minima are frequently encountered. To be confident of identifying the lowest variance for each configuration, it is necessary to employ all local grid minima as initial guess parameter values.

The analysis of these 6561 models, assuming that the intrinsic oxygen-binding affinities of α and β subunits in the tetramer are equal, involves estimating the optimal values for (1) the intrinsic tetramer subunit oxygen-binding free energy and (2) the intermediate state cooperative free energy for each of the possible three-state tetramer configurations. It should be noted that even though there are only 6561 different models, the grid search procedure identified a total of 18 741 possible relative minima for the Mills et al. data and 18 114 possible relative minima for the Chu et al. data. A least-squares parameter estimation was performed starting at each of these possible relative minima in order to be sure of finding all of the relative minima for the 6561 models. The best variance ratio obtained from the Mills et al. data is 1.45 and that from the Chu et al. data is 3.09 for the configuration 1223333333. Table I presents the constrained and derived parameter values for each data set. The variance ratios obtained indicate that this configuration does not represent an accurate characterization of system behavior. The four next best variance ratios obtained represent the same configurations (1323333333, 1233333333, 1223332333, and 1223323333) for each data set and increase rapidly in value to 3.81 for the Mills et al. data and to 9.40 for the Chu et al. data. The probability associated with these next best variance ratios is vanishingly small for each of the configurations identified for both data sets.

Further analysis was then performed on each of these configurations in which the rigidly constrained parameters are allowed to vary within their independently determined standard errors. Such analysis permits the parameter estimation algorithm to vary the values of the independently determined parameters to identify the variance minimum that may result in an improved variance ratio while only slightly altering the previously fixed parameter values. This is done to determine if small variations in the values of these independently determined parameters might lead to significantly improved variance ratios. This is critical for correct interpretation of the ability of any of these model-dependent configurations to accurately describe the data. Analysis performed in this manner yields a best variance ratio of 1.13 for the Mills et al. data and 1.74 for the Chu et al. data. Table II presents the derived parameter values with their approximate associated standard errors as determined for each data set. Relaxation of the rigid constraints permits variation in parameter values such that the data are substantially better approximated by the model and yielding a variance ratio for the Mills et al. data that cannot be eliminated by an F-test ($P < 18\%$). The analysis of the Chu et al. data indicates that this model is a significantly worse ($P < 0.0002\%$) description of the data than the model-independent thermodynamic analysis. The unliganded dimer to unliganded tetramer association free energy diverges from the independently determined value, but the derived error limits associated with this parameter overlap those obtained from the independent determination. However, the unliganded to fully liganded tetramer cooperative oxygen-binding free energy now assumes a value significantly in excess of that derived from independent measurements ($P < 0.5\%$ for the Mills et al. data and $P \sim 0$ for the Chu et al. data). The conclusion is thus supported that this three-state combinatorial switch configuration fails to accurately account for experimentally observed hemoglobin oxygen-binding behavior. The next best four configurations obtained from the rigidly constrained two parameter analysis (1323333333, 1233333333, 1223332333, and 1223323333) yield substantially higher variance ratios when analyzed in this way (up to 3.58 for the Mills et al. data and up to 8.41 for the Chu et al. data). The probability associated with these next best variance ratios is again vanishingly small for each of the configurations for both data sets ($P < 0.05\%$).

Table II: Statistically Constrained Parameter Analysis Results for the 1223333333 Configuration[a]

parameter	Mills et al. data	Chu et al. data
variance ratio	1.128	1.735
	$P \sim 18\%$	$P \sim 0.05\%$
$\Delta g_{21}' = \Delta g_{22}'$	−8.459 ± 0.050	−8.396 ± 0.055
$E(\alpha,\text{tet})$	−8.528 ± 0.040	−8.573 ± 0.045
$E(\beta-\alpha,\text{tet})$	0	0
$E(\text{coop},2)$	3.043 ± 0.028	3.051 ± 0.043
$E(\text{coop},3)$	6.834 ± 0.154	7.353 ± 0.179
	$P \sim 0.5\%$	$P \sim 0$
$^0\Delta G_2$	−14.688 ± 0.196	−14.737 ± 0.214

[a] Parameters are as defined for Table I; $E(\text{dimer})$, $E(\text{coop},3)$, and $^0\Delta G_2$ were constrained to be within 0.1 kcal of the values in Table I. Please note that these independently measured parameter values are constrained within a Gaussian distribution with a 0.1 standard deviation. This means that the parameter estimation procedure can force the actual value to be more than 0.1 from the optimal value, but in doing so the constraining procedure must pay a penalty of an increased variance ratio.

The analysis was also performed by fixing the independently determined parameter values and permitting the intrinsic oxygen-binding affinities of tetramer α and β subunits to vary independently. Optimal parameter values were then estimated for (1) the intrinsic tetramer α subunit oxygen-binding free energy, (2) the difference between the intrinsic tetramer β and α subunit oxygen-binding free energies, and (3) the intermediate tetramer cooperative free energy for each of the 6561

possible three-state tetramer configurations.

A total of 15251 possible relative minima were identified for the 6561 models for the Mills et al. data and a least-squares parameter estimation was performed for each of these starting values in order to find all of the relative minima. Only 131 of these least-squares parameter estimations yielded a variance ratio of less than 1.627 ($P < 0.02\%$) and thus might be considered a reasonable fit of the data. These 131 fits can be grouped into three categories. The first category was a single configuration, 1223333333, with three possible relative minima. Even though the grid search procedure had located three possible relative minima for this configuration, it was found that only a single minimum was reached by the least-squares parameter estimation procedure when it was started at these three different sets of initial values: $E(\alpha,\text{tet}) = -8.375$, $E(\beta-\alpha,\text{tet}) = -0.051$, $E(\text{coop},2) = 3.0201$, and variance ratio = 1.4499. This variance ratio corresponds to a probability of 0.22% that this model is equivalent to the model-independent thermodynamic analysis. The second category of configurations consisted of all possible combinations of the configuration $11sssst22s3$, where $s = 1$ or 2 and $t = 1$–3. A total of 64 possible relative minima was investigated for these 48 different configurations. The values of the estimated parameters were nearly identical for each of these 64 fits: $E(\alpha,\text{tet}) = -5.560 \pm 0.220$ (SD), $E(\beta-\alpha,\text{tet}) = -5.698 \pm 0.047$, $E(\text{coop},2) = 9.777 \pm 0.094$, and variance ratios ranging from 1.0182 to 1.2327. None of these models can be eliminated on the basis of the variance ratio since the highest variance ratio corresponds to a probability of about 10%. The third category of configurations consisted of all possible combinations of the configuration $1s1ss2ts23$, where $s = 1$ or 2 and $t = 1$–3. A total of 64 possible relative minima were investigated for these 48 different configurations. The values of the estimated parameters were nearly identical for each of these 64 fits: $E(\alpha,\text{tet}) = -11.169 \pm 0.040$, $E(\beta-\alpha,\text{tet}) = 5.514 \pm 0.077$, $E(\text{coop},2) = 9.674 \pm 0.104$, and variance ratios ranging from 1.0298 to 1.1521. None of these models can be eliminated on the basis of the variance ratio either.

The grid search analysis of the Chu et al. data yielded 14983 possible relative minima for the 6561 different models. When a least-squares analysis was performed starting at each of these 14983 sets of parameter values, only 65 were found with a variance ratio of less then 1.559 ($P < 0.02\%$). These 65 were the same as the third group of configurations of the Mills et al. data, e.g., all possible combinations of the configuration $1s1ss2ts23$, where $s = 1$ or 2 and $t = 1$–3. The values of the estimated parameters were nearly identical for each of these 65 fits: $E(\alpha,\text{tet}) = -10.795 \pm 0.035$, $E(\beta-\alpha,\text{tet}) = 4.946 \pm 0.069$, $E(\text{coop},2) = 9.497 \pm 0.104$, and variance ratios ranging from 1.2739 to 1.5149. These variance ratios correspond to probabilities of fit equivalent to the model-independent thermodynamic analysis of between 4% and 0.04%.

The analysis according to the first class of models, 1223333333, yielded an intermediate state cooperative free energy, $E(\text{coop},2)$, for both sets of data that was virtually identical with that found by Smith and Ackers (1985) in their cyanomet studies. However, the variance ratio was sufficiently high for the analysis of the Chu et al. data (variance ratio 3.088) to exclude this configuration as a possible description of hemoglobin cooperativity. The variance ratio from the Mills et al. data was also high, but not as significant.

The second and third classes of models yield variance ratios low enough that they appear to be satisfactory characterizations of oxygen-binding behavior as presented in the Mills et al. data. The analysis with the Chu et al. data, however, produces variance ratios suggesting a statistically invalid result for all three classes of models: 1223333333, $11sssst22s3$, and $1s1ss2ts23$. However, the confidence probability ($P < 4\%$) is not very high for the exclusion of the third class of models, $1s1ss2ts23$.

Model-independent thermodynamic analysis of the Chu et al. data yields a lower value of the variance than does the same analysis of the Mills et al. data. This is because of the presence of more experimental uncertainty in the Mills et al. data than in that of Chu et al. Thus, the Chu et al. data provide a more rigorous test for the model-dependent analysis that permits exclusion of these configurations and associated parameter values as satisfactory representations of the mechanism of hemoglobin oxygen-binding behavior.

The physical meaning of the determined parameters, $E(\alpha,\text{tet})$ and $E(\beta-\alpha,\text{tet})$, is also somewhat in doubt. The intrinsic free energy change for oxygen binding to the isolated α and β chains and to the α and β chains within an $\alpha\beta$ dimer is approximately −8.4 kcal/mol on the basis of a model-independent thermodynamic analysis (Mills et al., 1976; Chu et al., 1984). The analysis according to the third class of configurations, $1s1ss2ts23$, yielded values of the intrinsic free energy change for oxygen binding to the α chain within tetrameric hemoglobin, $E(\alpha,\text{tet})$, of −11.169 and −10.795 from the Mills et al. and Chu et al. data, respectively. The corresponding values for the β chain within the tetramer were −5.655 and −5.849, respectively. A small change in these quantities might be expected upon the association of the $\alpha\beta$ dimers to form tetrameric hemoglobin. However, it is not physically realistic for the interaction along the interface between the two $\alpha\beta$ dimers to be such that it increases the α chain free energy change for oxygen binding by −2.5 kcal/mol and at the same time introduces an equal and opposite change in the tetramer β chains. The net result is that the average affinity of the α and β chains within tetrameric hemoglobin is unchanged and the average value is the same as in isolated α and β chains and the chain values within dimers. It is much more likely that the search for a variance minimum has compensated for a physically unrealistic model by forcing the parameters of the model to have unrealistic values. The second class of models, $11sssst22s3$, introduces an approximately equal but opposite effect.

The value of the intermediate state cooperative energy, $E(\text{coop},2)$, is also in question in the analysis of oxygen-binding data. Smith and Ackers (1985) measured the intermediate state energy for cyanomethemoglobin to be approximately 3 kcal/mol. The conceptual basis of this quantity within the three-state combinatorial switch models is that it is an intermediate energy level between the values of $E(\text{coop},1)$ and $E(\text{coop},3)$, i.e., 0.0 and 6.33 kcal/mol. The value of approximately 9.6 kcal/mol determined for the second and third classes of configurations seems to be unrealistic. However, the reader should note that for oxygen binding to human hemoglobin, under these same experimental conditions, it has been experimentally observed that the last tetramer oxygen-binding step has a higher affinity than the isolated α and β chains and the $\alpha\beta$ dimer (Mills et al., 1976; Mills & Ackers, 1979; Chu et al., 1984). This "quaternary enhancement effect" was determined from a model-independent thermodynamic analysis and can thus be considered a model-independent experimental observation. The magnitude of the quaternary enhancement effect is approximately 0.5–1.0 kcal/mol. A consequence of the quaternary enhancement effect is that the intermediate state cooperative free energy, $E(\text{coop},2)$, might be slightly larger than the final state cooperative free energy,

Table III: Three-Parameter, Four-State Least-Squares Results for the 1223333334 Configuration[a]

parameter	Mills et al. data	Chu et al. data
variance ratio	0.986	1.002
$\Delta g_{21}' = \Delta g_{22}'$	−8.410	−8.323
$E(\alpha,\text{tet})$	−8.413 ± 0.002	−8.324 ± 0.002
$E(\beta-\alpha,\text{tet})$	0	0
$E(\text{coop},2)$	2.871 ± 0.029	2.747 ± 0.016
$E(\text{coop},3)$	6.653 ± 0.059	6.959 ± 0.074
$E(\text{coop},4)$	6.359	6.330
$^0\Delta G_2$	−14.437	−14.421

[a] Parameters are as defined for Table I; E(dimer), E(coop,4), and $^0\Delta G_2$ were fixed at the values from the model-independent thermodynamic analysis.

E(coop,3). However, the value of 9.6 kcal/mol calculated for the second and third class of models seems unrealistically large.

None of the comprehensive series of 6561 three-state combinatorial switch models that we have investigated are capable of simultaneously providing a good fit to the experimental data and physically meaningful model parameters. It thus can be concluded that *no* discrete three-state combinatorial switch model is a realistic description for the cooperative binding of oxygen by human hemoglobin.

Since no discrete three-state combinatorial switch configuration appears to accurately characterize hemoglobin oxygen-binding behavior, a brief survey was conducted to examine the feasibility of models based on discrete four-state combinatorial switch models. The tetramer configurations were modeled by allowing the fully liganded tetramer form to occupy cooperative energy state 4 characterized by the independently determined cooperative free energy of 6.3–6.4 kcal/mol (Mills et al., 1976; Chu et al., 1984). The unliganded tetramer form was constrained to occupy state 1 with zero cooperative free energy. The intermediate forms had distributions among states 2 and 3. Configuration 1223333333 is thus represented as 1223333334, for example. Independently determined parameters are rigidly constrained to their most probable derived values, and intrinsic tetramer subunit oxygen-binding free energies and the cooperative free energies of states 2 and 3 are permitted to vary. The presence of four accessible cooperative free energy states permits a statistically accurate description of the experimental data with the 1223333334 configuration while generating cooperative free energy values that are physically reasonable. The values presented in Table III correspond to the four-state model 1223333334 when $E(\beta-\alpha,\text{tet})$ is set to zero. The intrinsic affinity of the α and β chains within the tetramer, $E(\alpha,\text{tet})$ when $E(\beta-\alpha,\text{tet}) = 0$, has reasonable values for both data sets. The cooperative energy of the second step, E(coop,2), is approximately the 3 kcal/mol observed for the cyanomet case (Smith & Ackers, 1985). The value of E(coop,3) is approximately 0.5–1.0 more than E(coop,4), as would be expected in light of the quaternary enhancement effect (Mills et al., 1976; Mills & Ackers, 1979; Chu et al., 1984). The variance ratio is approximately unity, indicating that this model provides an excellent fit to both the Mills et al. data and the Chu et al. data. It thus appears that both sets of oxygen-binding data can be described by a discrete four-state combinatorial switch model. We have only presented one such four-state model, but we anticipate that many other four-state configurations exist that will also provide a reasonable description of the data.

It is interesting to note that the three-state configuration 1223333333, presented in Tables I and II, did not adequately describe the experimental data and that the four-state configuration 1223333334, presented in Table III, did adequately describe the data. The difference between these appears to be a requirement that the model be capable of describing an effect analogous to the quaternary enhancement effect before the model can adequately characterize the data.

It should be noted that the largest cross-correlation coefficient for the parameter estimations presented in Table III was 0.912 for the Mills et al. data and 0.890 for the Chu et al. data. These cross-correlation values are typical of all of the parameter estimations that we have presented. These values are sufficiently far from unity that the values of the parameters evaluated by the least-squares procedures are not interdependent; i.e., a large change in one of the parameters cannot be compensated for by a large change in another parameter with only a slight increase in the variance. Thus, the parameter estimation procedures should yield unique results.

The model as utilized in the present work does not permit equilibria among energy states to exist for any of the tetramer forms (Ferrone, 1986). The presence of such equilibria could effectively allow some forms of the tetramer to exhibit continuously variable average cooperative energies. Analytical treatment of a model of this type without additional constraints would require estimation of an unreasonably large number of parameters by the least-squares procedure.

We plan to extend our analysis to include a thorough survey of models based on discrete four-state combinatorial switch models. The failure of the present thorough survey of discrete three-state combinatorial switches to adequately characterize hemoglobin oxygen-binding behavior makes such an examination necessary. The preliminary identification of a discrete four-state combinatorial switch distribution capable of accurately describing hemoglobin oxygen-binding action suggests that a number of such statistically valid model-dependent configurations will be identified. A knowledge of the configurations and associated free energies of interaction characterizing oxygen- and protein-concentration-dependent hemoglobin action will provide enhanced understanding of the mechanisms involved in hemoglobin functional self-regulation. Such knowledge, in turn, will improve understanding of the principles involved in regulation of biological functions through mediation of functionally significant protein structural and energetic states.

Acknowledgments

We thank Dr. Gary K. Ackers for his advice and comments on this project and for the experimental data from his laboratory.

Appendix: Numerical Methods

Statistical Thermodynamic Formulation. The partition function for oxygen binding to hemoglobin tetramers may be expressed as (Johnson & Ackers, 1982)

$$\Xi_4 = \sum_i \sum_j g_{ij} \exp(-G_{ij}/RT)[\text{X}]^i$$

where G_{ij} is the free energy of the microscopic molecular configuration represented by the indices ij, i is the number of oxygens bound, j is the index to distinguish among different microscopic molecular configurations that have i oxygens bound, g_{ij} is the statistical degeneracy of configuration ij, R is the gas constant, T is the absolute temperature, and [X] is the concentration of unbound oxygen. The relative probabilities of each molecular species are thus represented by the Boltzmann distribution of the free energies for those species. A macroscopic analogue of the grand canonical partition function for a system comprised of n-mers with i ligands, ξ_{ni}, is defined as

$$\xi_{ni} = \sum_j g_{ij} \exp(-G_{ij}/RT)$$

The relationship between this subsystem partition function, ξ_{ni}, and the partition function for oxygen binding to tetramers yields

$$\Xi_4 = \xi_{40} + \xi_{41}[X] + \xi_{42}[X]^2 + \xi_{43}[X]^3 + \xi_{44}[X]^4$$

This permits definition of the product Adair oxygen-binding constants of tetramers as

$$K_{4i} = \xi_{4i}/\xi_{40}$$

Thus

$$\Xi_4 = 1 + K_{41}[X] + K_{42}[X]^2 + K_{43}[X]^3 + K_{44}[X]^4$$

The mean number of ligands bound by the tetramer, $\bar{N}_4$, may then be expressed as (Hill, 1960)

$$\bar{N}_4 = \frac{\partial \ln \Xi_4}{\partial \ln [X]} = \frac{\sum i K_{4i}[X]^i}{1 + \sum K_{4i}[X]^i} = \frac{Z_4'}{Z_4}$$

Analogous statistical thermodynamic development may be applied to hemoglobin dimers. Evaluation of the free energies of each microscopic configuration of dimers and tetramers then involves summation over all thermodynamic interactions relevant to each distinguishable species relative to a reference state. The values of the product Adair binding constants, K_{2i} and K_{4i}, obtained in this way together with knowledge of the unliganded dimer to unliganded tetramer association constant, ${}^0K_2$, may be used to generate the fractional saturation of hemoglobin, $\bar{Y}_{2,4}$, as a function of oxygen and protein concentration (Ackers & Halvorson, 1974).

Nonlinear Least-Squares Procedures. (*a*) *Nelder–Mead Parameter Estimation.* Application of the Nelder–Mead parameter estimation algorithm (Nelder & Mead, 1965) involves a multidimensional search for a minimum norm, e.g., variance, performed as a series of carefully selected one-dimensional searches. Determination of n parameter values requires that $(n + 1)$ sets of parameters be selected such that they define an n-dimensional simplex. In the present work, n mutually orthogonal simplex vertices are generated such that the centroid (arithmetic mean) of these vertices corresponds to the initial guess of the parameter values. The variance is then evaluated at each of the simplex vertices. The vertex with the largest variance is identified, and the centroid of the remaining vertices is determined. A one-dimensional search is then conducted along the line in n-dimensional parameter space defined by (1) the vertex determined to have the largest variance and (2) the centroid of the remaining vertices. This search is conducted to identify parameter values that correspond to a variance which is lower in value than that of at least two of the simplex vertices. The point of the original simplex corresponding to the largest variance is then replaced with the parameter values defining the newly identified point. A new simplex is thus generated, and this procedure is repeated until all $(n + 1)$ simplex vertices have associated variances within some specified range of values, the criterion for convergence. In the present work, convergence is assumed when the fractional range in variance is less than 10^{-5} of the mean value of the variances associated with the simplex vertices. All points of the simplex are thus defined by parameter values that correspond to effectively equivalent values of the variance. The values associated with the vertex with the minimum variance are then reported as those defining that particular minimum in variance space.

(*b*) *Gauss–Newton Parameter Estimation.* A modified Gauss–Newton parameter estimation algorithm is applied to selected tetramer configurations and their optimal parameter values as derived from the extensive grid search and Nelder–Mead procedure to confirm them by an independent method and to generate approximate confidence limits for the parameters. The details of this algorithm are presented elsewhere (Johnson & Frasier, 1985). Briefly, a function, G, of the independent variable(s), X_i, and the parameters being estimated, α, are chosen to directly approximate the experimental data, Y_i, such that $Y_i = G(X_i,\alpha)$. No transforms of the experimental data are employed (e.g., as in a Hill plot) because of the potential for introducing nonlinear distortions upon the distribution of random experimental error. Such nonlinear transforms invalidate the assumption of Gaussian distributed experimental error such that the usual least-squares criterion may no longer be applied. In addition, the parameters comprising the vector α should, in general, be the actual parameters that are of interest, not related, transformed parameters.

Given some set of initial guess parameter values, partial derivatives of the function G are evaluated with respect to each variable parameter, α_j, to generate a matrix P with elements P_{ij} as

$$P_{ij} = \partial G(X_i,\alpha)/\partial \alpha_j$$

and a vector of residuals, Y^*, is generated with elements Y_i^* as

$$Y_i^* = Y_i - G(X_i,\alpha)$$

A vector ϵ is then determined such that

$$\epsilon = (P'P)^{-1}P'Y^*$$

$$P' = \text{transpose of } P$$

$$(P'P)^{-1} = \text{inverse of } (P'P)$$

The basic Gauss–Newton procedure then provides α^k as

$$\alpha^k = \alpha^{k-1} + \epsilon$$

where α^k is the value of α for the kth iteration. The procedure is continued until the fractional change in α is less than some specified tolerance limit.

A modification is made in this basic algorithm in that ϵ is used to estimate direction only, instead of direction and distance, and a search is performed to find the distance necessary to generate a minimum variance. The magnitude of α is changed by factors of 2 until two consecutive sets of parameter values are obtained that (1) have a corresponding variance less than that of the previous vector and (2) have a corresponding variance greater than that of the previous vector. The values of α from the previous iteration and those from these two newly identified parameter vectors are then used to derive a quadratic polynomial. The derivative of the resulting polynomial is used to estimate parameter values that correspond to a minimum variance. If the variance associated with one of the original three vectors is lower than that of the predicted minimum, the values defining the vector with the lowest variance are taken. This procedure is continued until the fractional change in the variance is less than some specified tolerance limit. In the present work, iterations are continued until the fractional change in variance is 10^{-6} or less. Such a stringent convergence criterion is employed to most rigorously identify the minimum of the variance.

(*c*) *Constraining the Parameter Estimation Process.* In the extensive, multiconfiguration analysis, conducted by application of the grid search followed by Nelder–Mead parameter estimation, values for free energy parameters determined from independent analysis are rigidly constrained to their most probable derived values. These parameters are the unliganded dimer to unliganded tetramer association free energy, the free energies for binding the first and second oxygens to dissociated

dimers, the cooperative free energy of the unliganded tetramer, and the cooperative free energy of the fully liganded tetramer. Such rigid constraint of independently derived parameter values makes it necessary to estimate only the intrinsic tetramer α and β subunit oxygen-binding free energies and the intermediate tetramer cooperative oxygen-binding free energy as variable parameters. Estimating only these parameters greatly reduces the computation time required to examine all possible discrete three-state combinatorial switch configurations.

For the configurations that yield the lowest variances as identified above, further analysis is performed permitting the independently determined parameters to vary within statistically constrained limits. The values of the independently determined parameters, along with their derived approximate standard errors, are included as additional data points in the fractional oxygen saturation data files. Upon encountering the newly included data points, the parameter estimation algorithm employs a different set of functions, G, for characterization of the corresponding input values and their associated standard errors. Inclusion of this capability into the parameter estimation algorithm permits the independently determined parameters to deviate from their most probable values while constraining the magnitude of any deviation by the statistical weighting factor, the approximate standard error. The variance is calculated so as to simultaneously account for the oxygen-binding data and the statistically constrained parameters. The derived variance thus accurately represents contributions from all relevant constraints pertaining to experimental uncertainty and all constraints are simultaneously accounted for in a statistically valid manner.

(*d*) *Confidence Interval Estimation.* Estimates of confidence intervals around variable parameters is possible by employing the modified Gauss–Newton algorithm in analysis. The details of this method for estimating confidence intervals in nonlinear, asymmetric variance spaces is discussed by Johnson (1983). Briefly, the procedure involves searching the variance space for an F-statistic corresponding to 67% confidence probability. This corresponds to approximately one standard deviation for a Gaussian distribution. This search of variance space is performed in two ways. (1) The elements of the parameter vector, α, are varied independently. (2) The direction of the search is defined in terms of the F-statistic as the axis of the multidimensional hyperellipsoid generated by the solutions, Ω, of the equation

$$(\alpha - \Omega)PP'(\alpha - \Omega) < n\sigma^2 F\text{-statistic}$$

where n is the number of parameters and σ^2 is the variance of the minimum.

Because of correlation among successive data points, correlation among estimated parameters, and nonlinearity of the equations, the derived confidence limits are only approximate estimates of the true values. Confidence limits derived in this way are usually asymmetric and are thus reported as lower and upper bounds by the fitting algorithm. However, in the present work, the extent of observed asymmetry was not substantial, so all confidence intervals are reported as plus and minus the range obtained by dividing the derived range by 2. The standard deviations derived in this way do not necessarily indicate the accuracy of the experimental parameters, because the validity of the particular mathematical formulation is implicit in such an interpretation. They do, however, indicate the quality of a given model-dependent fit relative to the uncertainty encountered in the experimental data being analyzed and to all relevant mathematical correlations that may exist.

Registry No. O_2, 7782-44-7.

REFERENCES

Ackers, G. K. (1980) *Biophys. J. 32*, 331–346.

Ackers, G. K., & Halvorson, H. R. (1974) *Proc. Natl. Acad. Sci. U.S.A. 71*, 4312–4316.

Ackers, G. K., & Johnson, M. L. (1981) *J. Mol. Biol. 147*, 559–582.

Ackers, G. K., & Smith, F. R. (1987) *Annu. Rev. Biophys. Chem. 16*, 583–609.

Asher, S. A., Adams, M. L., & Schuster, T. M. (1981) *Biochemistry 20*, 3339–3346.

Baldwin, J., & Chothia, C. (1979) *J. Mol. Biol. 129*, 175–220.

Chu, A. H., Turner, B. W., & Ackers, G. K. (1984) *Biochemistry 23*, 604–617.

Eisenberger, P., Shulman, R. G., Kincaid, B. M., Brown, G. S., & Ogawa, S. (1978) *Nature (London) 274*, 30–34.

Ferrone, F. A. (1986) *Proc. Natl. Acad. Sci. U.S.A. 83*, 6412–6414.

Flanagan, M. A., Ackers, G. K., Matthew, J. B., Hanania, G. I. H., & Gurd, F. R. N. (1981) *Biochemistry 20*, 7439–7449.

Hill, T. L. (1960) *Introduction to Statistical Mechanics*, Addison-Wesley, Reading, MA.

Johnson, M. L. (1983) *Biophys. J. 44*, 101–106.

Johnson, M. L. (1986) *Biochemistry 25*, 791–797.

Johnson, M. L., & Ackers, G. K. (1982) *Biochemistry 21*, 201–211.

Johnson, M. L., & Frasier, S. G. (1985) *Methods Enzymol. 117*, 301–342.

Johnson, M. L., Halvorson, H. R., & Ackers, G. K. (1976) *Biochemistry 15*, 5363–5371.

Johnson, M. L., Turner, B. W., & Ackers, G. K. (1984) *Proc. Natl. Acad. Sci. U.S.A. 81*, 1093–1097.

Mills, F. C., & Ackers, G. K. (1979) *Proc. Natl. Acad. Sci. U.S.A. 76*, 273–277.

Mills, F. C., Johnson, M. L., & Ackers, G. K. (1976) *Biochemistry 15*, 5350–5362.

Nelder, J. A., & Mead, R. (1965) *Comput. J. 7*, 308–313.

Perutz, M. F. (1970a) *Nature (London) 228*, 726–734.

Perutz, M. F. (1970b) *Nature (London) 228*, 734–739.

Perutz, M. F., Muirhead, H., Mazzarella, L., Crowther, R. A., Greer, J., & Kilmartin, J. V. (1969) *Nature (London) 222*, 1240–1243.

Pettigrew, D. W., Romeo, P. H., Tsapis, A., Thillet, J., Smith, M. L., Turner, B. W., & Ackers, G. K. (1982) *Proc. Natl. Acad. Sci. U.S.A. 79*, 1849–1853.

Russu, I. N., Ho, N. T., & Ho, C. (1983) *Biochemistry 22*, 5031–5043.

Smith, F. R., & Ackers, G. K. (1985) *Proc. Natl. Acad. Sci. U.S.A. 82*, 5347–5351.

Szabo, A., & Karplus, M. (1972) *J. Mol. Biol. 72*, 163–197.

Viggiano, G., & Ho, C. (1979) *Proc. Natl. Acad. Sci. U.S.A. 76*, 3673–3677.

Viggiano, G., Ho, N. T., & Ho, C. (1979) *Biochemistry 18*, 5238–5247.